


RESEARCH

Open Access



Analysis of grounding system transient with consideration of soil ionization and mutual coupling effect

Kaushal Pratap Sengar^{1*}  and Kandasamy Chandrasekaran²

*Correspondence:
kaushalsengar786@gmail.com

¹ Department of Electrical Engineering, Madhav Institute of Technology and Science, Gwalior, M.P., India

² Department of Electrical Engineering, National Institute of Technology, Raipur, C.G., India

Abstract

The grounding system of an electrical substation provides safety to both operator and equipment. The lightning current waveform has a major influence on the dynamic performance of ground electrodes. If lightning current is large enough, soil will be ionized, which will have a great effect on the transient performance of the grounding system. Many numerical models have been developed to evaluate the transient performance of grounding system, still it is a challenging task to analyze the impulse behavior of grounding system efficiently. In this paper, the transient behavior of grounding systems with consideration of nonlinear and dynamic effects of soil ionization is presented. Grounding systems such as vertical rod, horizontal conductor and grounding grid buried in the homogeneous soil are considered as case study. Proposed model is the combination of circuit theory approach and method of moment with consideration of frequency-dependent impedance and mutual coupling effect between the conductor segments. Self and mutual component of inductance and resistance are considered in the analysis. Initially, transient performance of grounding system is analyzed for single vertical rod, horizontal and square grounding electrodes, further it is extended for vertical rod (more than one), horizontal conductor and grounding grids with different configurations. The analysis of grounding system with the consideration of mutual coupling effect is compared with devoid of mutual coupling, and differences between them are evaluated. For validating the developed method, simulated results are compared with the results reported in the literature, and good agreements are found. Analysis shows that the grounding impulse impedance decreased with increasing the magnitude of injected current. Developed method will help to improve the modeling of simple as well as complex grounding system buried in homogeneous soil.

Keywords: Grounding system, Impulse impedance, Leakage current, Soil ionization, Transient voltage

Introduction

The grounding system using vertical rods, horizontal conductors and grounding grid provides a low-impedance path and ensure smooth distribution of ground potential, developed due to high magnitude fault or lightning current [1]. An effective grounding system disperses abnormal current into the ground without increase the ground

potential and induced voltage that might be danger to the operators, installations and equipment [2]. The grounding system for high voltage substation should be designed to meet both safe and economic conditions [3, 4]. Grounding system performance under normal and fault conditions are well understood in [5], but the dynamic behavior of grounding electrode associated with lightning return stokes has different characteristics from low frequency because of soil ionization and conductor reactance [6, 7]. The transient performance of grounding system was analyzed by experimental work in [8, 9] and by numerical methods such as method of moment (MoM) in [10], finite difference time domain (FDTD) in [11], finite element method (FEM) in [12] and partial element equivalent circuit (PEEC) in [13]. The representation of grounding conductor as equivalent impedance is necessary due to the frequency contents of lightning current that makes reactive effect vary relevant. Studies reported in [14, 15] show that with high magnitude of leakage current, impulse impedance of grounding electrode decrease. Under the influence of high magnitude impulse current, an electric field surrounding the grounding electrode goes beyond to the critical breakdown limit of soil and ionization occurs [16]. In fact, transient phenomenon depends on geometrical and electrical parameters of grounding system such as shape and size of the electrode, soil resistivity in addition to rise time, decay time and peak of the injected current impulse [17, 18]. In [19, 20], the grounding impedance of the grounding grid shows a downward trend with the increase in impulse current amplitude. Also in [21], the tower footing impedance was found to have a high reduction when the lightning current increased. Several numerical simulations and testings are mainly focused to study the impulse behavior of grounding system [22, 23]. Different models such as circuit model, electromagnetic field model (EMF) and transmission line model (TLM) are developed to compute the transient behavior of grounding electrodes under lightning current energization condition. In circuit model [24, 25], grounding electrode is represented as a lumped RLC circuit. This model can incorporate soil ionization phenomenon, but it is difficult to deal with frequency-dependent parameters. In [26, 27], a new model is developed from the equation of nonuniform transmission lines (nuTL), which takes into account the electromagnetic couplings that arise after spatial discretization and soil ionization of grounding system. Electromagnetic field model [28, 29] is based on Maxwell's equations. This model is frequency-domain approach and limited only for linear circuits. In [30], a model is developed which allows complete electromagnetic study by Finite Element Method (FEM) of a grounding system in the significant frequently spectrum of a lightning stroke or a short circuit. The electromagnetic approach based on antenna theory and the method of moments (MOMs) is presented in [31]. This model is a full-wave frequency-domain approach and based on Hertzian dipole with a lossy half-space. Therefore, this method is not suited for the modeling of nonlinear phenomena but well suited for modeling frequency-dependent characteristics [31, 32]. In TLM [33, 34], impulse response of grounding electrode is similar to the wave-propagation of transmission lines. This method is not capable to incorporate the mutual phenomenon between grounding electrodes. Transient response of grounding system in multilayer soil structure is analyzed using PEEC technique using quasi-static complex image method in [35]. The full-wave computational solution based on method of moments (MoM) is adopted to investigate the transient behavior of substation grounding system [36]. In

[37], transient analysis on wind farms with interconnected grounding systems is analyzed using partial element equivalent circuit (PEEC). However, many numerical models have been developed to analyze the transient performance, still it is challenging task to predict the impulse behavior of grounding system efficiently. From the related literature, it is found that there is scope to improve the transient model of grounding system under the consideration of mutual effects between conductor segments and frequency-dependent parameters.

This paper presents a modified numerical method based on MoM and circuit theory approach to analyze the transient behavior of grounding systems with consideration of soil ionization phenomenon. The developed model also includes mutual coupling between the conductor segments and frequency-dependent impedance of grounding electrodes. The validation of developed method has been done by comparing the calculated results with the published results reported in the literature for vertical rod, horizontal grounding conductor and square grounding electrode. The study is also extended to simulate the transient voltage for complex grounding system with and without consideration of soil ionization phenomenon. Percentage relative difference is evaluated between the grounding models with and without consideration of mutual coupling. The model applications are proved reliable to perform the transient analysis and soil ionization phenomenon in the presence of high magnitude impulse current.

Grounding system analysis

Grounding system is analyzed in frequency domain using MoM and circuit theory approach because of unbalanced distribution of the current in the grounding electrode as in [6]. Method used in this paper incorporates conductive, inductive and capacitive couplings between the electrode segments. The grounding electrodes are divided into number of segments. Each segment is considered as a branch of the circuit that is formed by series resistance, self and mutual inductance. The segment length is taken as 1/10 of the wavelength in the soil. Impulse current with higher frequency and different magnitude is injected at one node of the grounding circuit to energize it. Distribution of the current is arranged on the basis of MoM [38] by considering a grounding electrode with k segments and n nodes. Circuit theory approach is used to develop the nodal incidence matrix. When impulse current is injected at one or more nodes, electric current flows through the grounding electrodes and some part of the current leaks into surrounding soil. There are two longitudinal current: One is at starting point of the segment and other is at the end point of the segment. It is considered that the longitudinal current from starting point to central point of the segment is uniform and equal to the starting point current. Similarly current from central point to the end point is uniform and equal to the central point current. It is assumed that the longitudinal current I_l^- and I_l^+ are centralized in the axis, and leakage current I_e is flowing out from the middle of the segment (central node) into the soil. Hence, the whole circuit is converted into $2k$ branches and $n + k$ nodes. The surface potential (ϕ_c) at the central node of the segment is developed due to the leakage current of each segment and given using (1)

$$[\phi_c] = [R][I_e] \quad (1)$$

here R is resistance matrix of the grounding network. The diagonal elements of resistance matrix are self-resistance related with the central nodes, and the off-diagonal elements are mutual resistance. The self-resistance is defined as the potential at the corresponding node, when a unit current leaks radially into the soil. The mutual resistance between two middle nodes associated with the segment is defined as the potential on the node when a unit leakage current is flowing radially into the soil from another central node. For four central nodes, the grounding network can be represented using dependent and independent voltage sources as in Fig. 1.

If leakage current I_{e1} flows into the soil from central node C_1 , the potential of the central points C_1 to C_4 will be $\phi_{11}, \phi_{21}, \phi_{31}, \phi_{41}$. For only leakage current I_{e2} flowing from central node C_2 , the potential of the central points C_1 to C_4 will be $\phi_{12}, \phi_{22}, \phi_{32}, \phi_{42}$. Similarly for leakage current I_{e3} , potential will be $\phi_{13}, \phi_{23}, \phi_{33}, \phi_{43}$ and for leakage current I_{e4} , potential will be $\phi_{14}, \phi_{24}, \phi_{34}, \phi_{44}$. Total potential on the central point of j th segment for leakage currents of i number of segments, due to self and mutual resistance can be represented using (2):

$$\phi_j = \sum_{i=1}^k R_{ji} I_{ei} \tag{2}$$

$$i = 1, 2, 3, \dots, k$$

R is the resistance matrix that includes the self and mutual ground coupling between the conductor segments. $R_{j,i}$ is self-resistance for $i = j$, and $R_{j,i}$ is mutual resistance for $i \neq j$. The relation between column matrix $[\phi_c]$ of the potential on the surface of branch and leakage current matrix $[I_e]$ can be represented using (3):

$$[I_e] = [R]^{-1}[\phi_c] = [G][\phi_c] \tag{3}$$

where $[G]$ is a matrix of conductive and capacitive coefficients. “The capacitive reactance among the electrode segments is also incorporated in the analysis.” Soil is considered

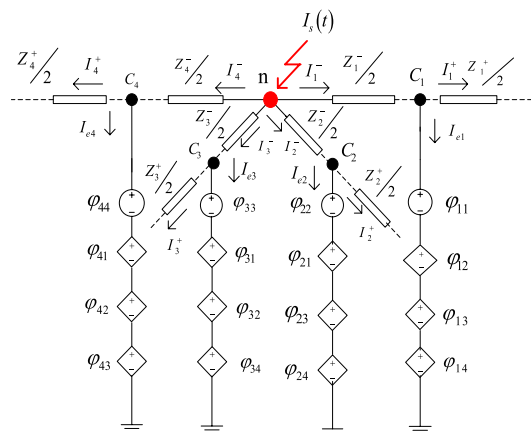


Fig. 1 Grounding grid portion with nodes and segments. Where $\phi_{11} = R_{11}I_{e1}, \phi_{12} = R_{12}I_{e2}, \phi_{13} = R_{13}I_{e3}, \phi_{14} = R_{14}I_{e4}; \phi_{22} = R_{22}I_{e2}, \phi_{21} = R_{21}I_{e1}, \phi_{23} = R_{23}I_{e3}, \phi_{24} = R_{24}I_{e4}; \phi_{33} = R_{33}I_{e3}, \phi_{31} = R_{31}I_{e1}, \phi_{32} = R_{32}I_{e2}, \phi_{34} = R_{34}I_{e4}; \phi_{44} = R_{44}I_{e4}, \phi_{41} = R_{41}I_{e1}, \phi_{42} = R_{42}I_{e2}, \phi_{43} = R_{43}I_{e3}$

as a semi-infinite medium, and it has different conductivity and permittivity compared to the air, so the principle of image method can be used to calculate the ground resistance parameters [39]. The potential at the central point of the segments is represented with the transverse conductance. It represents the leaking current from the grounding electrode into the soil and is a function of soil property and the electrode geometry. The coefficient of potential on segment i due to leakage current from the segment j is given using (4)

$$R_{ij} = \frac{1}{4\pi(\sigma_g + j\omega\epsilon_g)l_i} \cdot \left[\int_{\Gamma_i} \int_{\Gamma_j} \frac{1}{d_{ij}} dl_i dl_j + \alpha_g \cdot \int_{\Gamma_i'} \int_{\Gamma_j} \frac{1}{d_{i'j}} dl_{i'} dl_j \right] \tag{4}$$

where α_g is reflection coefficient and given as:

$$\alpha_g = \frac{\sigma_g + j\omega(\epsilon_g - \epsilon_0)}{\sigma_g + j\omega(\epsilon_g + \epsilon_0)}$$

σ_g and ϵ_g are the conductivity and permittivity of the soil, respectively. $\Gamma_{i'}$ is the segment image of i' ; $d_{i'j}$ is the distance between segment image i' in the air and segment j in the ground. The admittance matrix $[G_{ij}]$ is obtained by inverse matrix of $[R_{ij}]$ using (5):

$$[G] = [R]^{-1} \tag{5}$$

For reactance calculation, it is assumed that air and soil are nonmagnetic materials and they have the same permeability μ_0 . The longitudinal current segments of the grounding electrode are represented with longitudinal impedances. The longitudinal impedance matrix of the grounding system with $2k$ branches and $k + n$ nodes is evaluated using (6) as in [17]:

$$Z = \begin{bmatrix} Z_{1,1} & \cdots & Z_{1,i} & \cdots & Z_{1,2k} \\ \vdots & & \vdots & & \vdots \\ Z_{i,1} & \cdots & Z_{i,i} & \cdots & Z_{i,2k} \\ \vdots & & \vdots & & \vdots \\ Z_{2k,1} & \cdots & Z_{2k,i} & \cdots & Z_{2k,2k} \end{bmatrix} \tag{6}$$

$$Z_{i,i} = Z_0 + j\omega M_{i,i} \quad i = 1, 2, \dots, 2k \quad \omega = 2\pi$$

where Z_0 is an internal impedance, it is a frequency-dependent parameter due to skin effect. The self-impedance $Z_{i,i}$ is made up with internal impedance Z_0 and external impedance $j\omega M_{i,i}$. Because of segment current is not properly distributed over the cross section of the conductor due to skin effect, frequency variant equation is used to calculate the internal impedance. For a solid circular conductor with radius ' a ', the internal impedance of the grounding electrode is calculated using (7) as given in [40, 41].

$$Z_0 = \frac{j\omega\mu I_0(\gamma_a)}{2\pi a\gamma I_1(\gamma_a)} \tag{7}$$

$$\gamma = \sqrt{j\omega\mu/\rho_c}$$

where μ is permeability, ρ_c is conductor resistivity, $I_0(\gamma_a)$ is zero order Bessel's function, $I_1(\gamma_a)$ is first order Bessel's function and f is the grounding current frequency. External impedance $j\omega M_{i,i}$ of any electrode segment can be calculated using surface current of the segment as given in [42]. Mutual reactance between two segments is determined by filament model and can be represented using (8) as in [13, 43].

$$Z_{i,j} = j\omega \frac{\mu_0}{4\pi} \int_{l_i} \int_{l_j} \frac{\vec{dl}_i \cdot \vec{dl}_j}{D_{ij}} \tag{8}$$

For two parallel segments with spacing d_0 and length l_0 , mutual reactance can be calculated using (9)

$$Z_{i,j} = j\omega \frac{\mu_0 l_0}{4\pi} \left[\ln \left(\frac{l_0}{d_0} + \sqrt{1 + \frac{l_0^2}{d_0^2}} \right) - \sqrt{1 + \frac{d_0^2}{l_0^2}} + \frac{d_0}{l_0} \right] \tag{9}$$

if incidence matrix of the grounding circuit node is $[A]$, than, nodal admittance matrix can be evaluated using (10) as given in [44].

$$[Y]_{k+n} = [A][Y][A]^T, [Y] = [Z]^{-1} \tag{10}$$

where $[Y]$ is nodal admittance matrix that includes resistive and inductive effects. Nodal potential matrix $[\phi_n]$ is obtained using (11), and admittance matrix of the nodes is given by $[Y]_{k+n}$.

$$[Y]_{k+n} \begin{bmatrix} \phi_c \\ \phi_n \end{bmatrix} = \begin{bmatrix} -I_e \\ I_s \end{bmatrix} \tag{11}$$

From (3) and (11)

$$[Y]_{k+n} \begin{bmatrix} \phi_c \\ \phi_n \end{bmatrix} + \begin{bmatrix} G & 0 \\ 0 & 0 \end{bmatrix} \begin{bmatrix} \phi_c \\ \phi_n \end{bmatrix} = \begin{bmatrix} 0 \\ I_s \end{bmatrix}$$

$$\left\{ [Y]_{k+n} + \begin{bmatrix} G & 0 \\ 0 & 0 \end{bmatrix} \right\} \begin{bmatrix} \phi_c \\ \phi_n \end{bmatrix} = \begin{bmatrix} 0 \\ I_s \end{bmatrix}$$

Square matrix of $(k + n)$ order is divided into four parts

$$\left\{ \begin{bmatrix} Y_{kk} & Y_{kn} \\ Y_{nk} & Y_{nn} \end{bmatrix} + \begin{bmatrix} G & 0 \\ 0 & 0 \end{bmatrix} \right\} \begin{bmatrix} \phi_c \\ \phi_n \end{bmatrix} = \begin{bmatrix} 0 \\ I_s \end{bmatrix}$$

$$\begin{bmatrix} Y_{kk} + G & Y_{kn} \\ Y_{nk} & Y_{nn} \end{bmatrix} \begin{bmatrix} \phi_c \\ \phi_n \end{bmatrix} = \begin{bmatrix} 0 \\ I_s \end{bmatrix}$$

where Y_{kk} and Y_{nn} are k order and n order matrix, respectively. Y_{nk} is n rows and k columns matrix, and Y_{kn} is k rows and n columns matrix. $[I_s]$ is a column matrix of the injected current at node. $[I_s]$ is represented using (12)

$$[I_s] = [I_s, 0, 0, 0]^T \quad (12)$$

Grounding electrode is divided into N segments. Consider m, m^-, m^+ are the central and two end points of the segment m ($m = 1, 2 \dots N$), respectively. According to the developed model leakage current, $I_{e,m}$ can be expressed as (13) as in [10]

$$I_{e,m} = I_{l,m^-} - I_{l,m^+} \quad (13)$$

Longitudinal current flowing through the segment's two end I_l^- and I_l^+ can be obtained from $[\phi_c]$ and $[\phi_n]$ using (14) and (15), respectively [6].

$$[I_l^-] = \frac{([\phi_c] - [C_0][\phi_n])}{[Z]} \quad (14)$$

C_0 is known as relation matrix. It represents the relationship between node and starting point of the segment. If starting point of segment j is connected to node i , then, $C_{0j,i}$ is one otherwise zero.

$$[I_l^+] = \frac{([C_1][\phi_n] - [\phi_c])}{[Z]} \quad (15)$$

C_1 is a relation matrix reflects the relationship between node and end point of the segment, if end point of segment j is connected to the node i , then, $C_{1j,i}$ is one otherwise zero. $[\phi_c]$ and $[\phi_n]$ are potential matrix at the surface of the segment and nodes, represented in (16) and (17), respectively.

$$[\phi_c] = [\phi_{c1}, \phi_{c2}, \phi_{c3}, \phi_{c4}]^T \quad (16)$$

$$[\phi_n] = [\phi_{n1}, \phi_{n2}, \phi_{n3}, \phi_{n4}]^T \quad (17)$$

The relation between leakage current I_e and current flowing between the two ends of the segments can be calculated using (18):

$$[I_e] = [I_l^-] - [I_l^+] \quad (18)$$

Modeling of soil ionization

Soil breakdown occurs if high magnitude current is applied on buried grounding electrode and electric field (E) surrounding the grounding electrode exceeds the critical electric field (E_c) of the soil. Several studies have been carried out to analyze the breakdown mechanism of soil and suggested E_c for different type of soil models [14, 45–47]. Soil becomes a good conductor during $E > E_c$. The critical electric field of soil can be calculated using (19)

$$E_c = 241\rho^{0.215} \quad (19)$$

where ρ is soil resistivity in $\Omega.m$. Generated electric field E is a function of soil resistivity and the radius of grounding electrode. It is calculated using (20)

$$E = \rho I_e / (2\pi al) \quad (20)$$

For soil ionization

$$E > E_c$$

$$E = \alpha E_c (\alpha \geq 1) \quad (21)$$

α is a coefficient that depends on transient current and soil resistivity as in [37].

From (21)

$$\frac{\rho I_e}{2\pi al} = \alpha \times 241 \rho^{0.215}$$

$$\alpha.a = \rho^{0.785} \times I_e / 481\pi l \quad (22)$$

At the instant when electric field E exceeds the critical value E_c , the equivalent radius of conductor during soil ionization is calculated using (23):

$$a_i = a \frac{E}{E_c} \quad (23)$$

Using (21), Eq. (23) is modified as (24)

$$a_i = a \frac{\alpha E_c}{E_c}$$

$$a_i = \alpha.a \quad (24)$$

From (22) and (24), equivalent radius of grounding electrode can be obtained using (25)

$$a_i = \rho^{0.785} \times I_e / 481\pi l \quad (25)$$

Figure 2a represents the soil ionization phenomenon surrounding the electrode, and Fig. 2b represents the procedure to perform the transient analysis of grounding system with consideration of soil ionization phenomenon in the form of flowchart.

The assumptions made in this paper for soil ionization modeling are as follows:

1. Leakage current I_e leaks from per unit length of a cylindrical conductor to the earth. When E exceeds to E_c on conductor surface, soil ionization starts on surrounding earth of the conductor. The radius of the conductor exceeds up to the point where E decrease to E_c . The ionized zone has cylindrical shape and concentric with the conductor.
2. The self and mutual inductance of the conductors are not affected due to soil ionization phenomenon. Ionization phenomenon is modeled with above mentioned

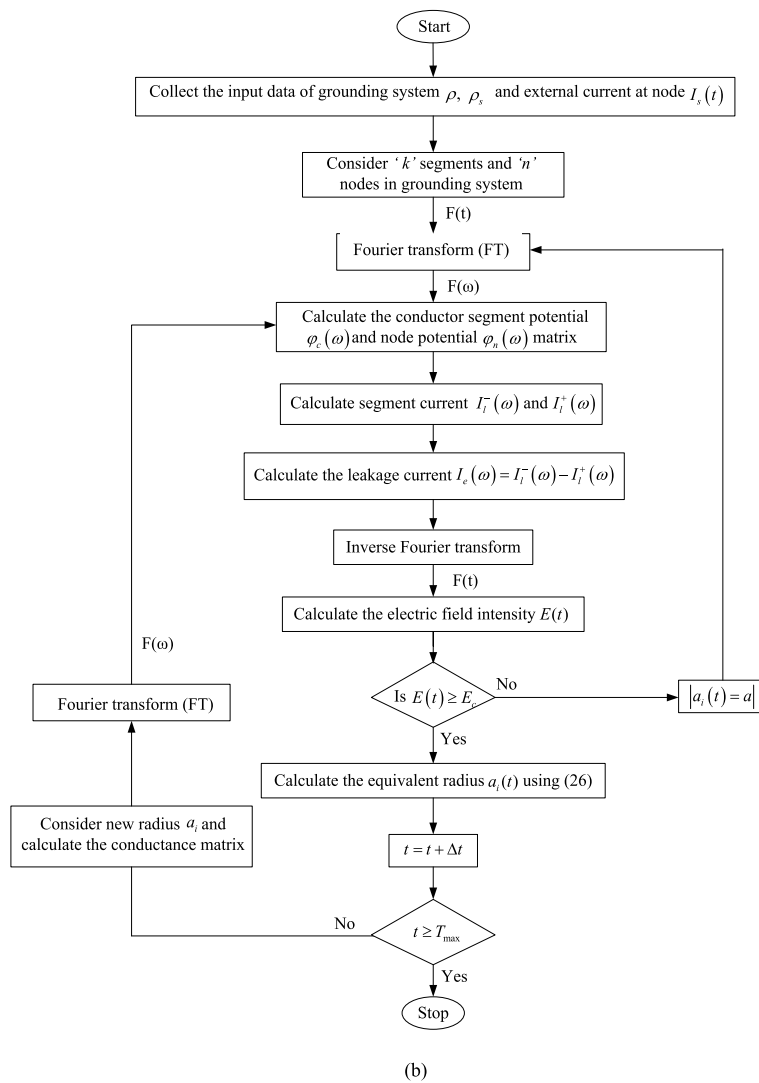
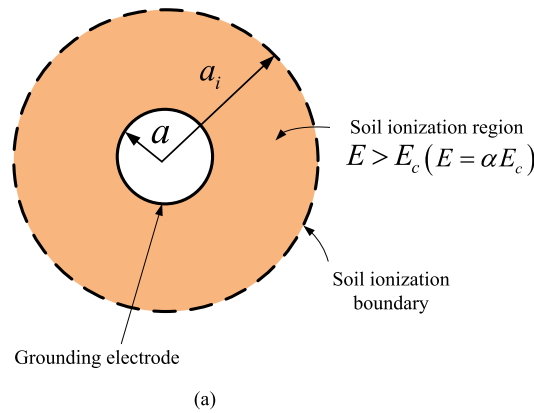


Fig. 2 **a** Soil ionization surrounding the grounding electrode. **b** Proposed flowchart for transient analysis of grounding system

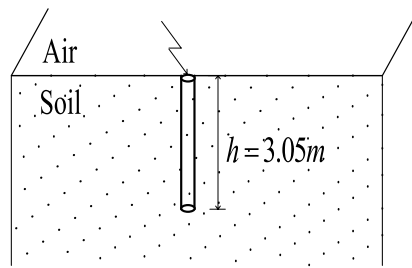


Fig. 3 Single vertical grounding rod under homogenous soil

assumptions and appropriate modifications are done in the conductor radius. Hence, conductance matrix $[G]$ is recalculated with modified radius for verifying $E > E_c$.

- When high magnitude current is injected at the nodes of grounding network, a time dependent current function $I(t)$ is determined. Using Fourier transform, time dependent current function is converted into the frequency domain as $I(\omega)$. Also, nodal potential $\phi_n(\omega)$, branch surface potential $\phi_c(\omega)$ and leakage current $I_e(\omega)$ are computed to solve the system in frequency domain. Using inverse Fourier transform, the leakage current $I_e(t)$, potential $\phi_c(t)$, $\phi_n(t)$ and electric field $E(t)$ are determined. System may be unstable due to update its parameters in frequency domain in each time step, so the effective method is needed to transform the transient impulse from time domain to frequency domain as in [48]. Critical electric field for soil breakdown is assumed to be 300 kV/m as suggested in [14]. With consideration of factious radius a_i , the each electrode at every instant conductance matrix $[G]$ is computed using (26)

$$[G'(t)] = [G(t)] + [\Delta G] \quad (26)$$

Validation of the method

Validation with Liew and Darveniza [14]

The method used in this paper is verified for vertical copper rod with 3.05 m length and 5 mm radius, buried in homogenous soil model with different soil resistivity as shown in Fig. 3. A $4 \mu\text{s}$ time-to-peak ramp current is injected at the top of the grounding rod, and impulse impedance is calculated for different current peaks. The value of critical electric field E_c is considered as 300 kV/m. Figure 4a, b depicts the results of impulse impedance for different impulse current peak. Impulse impedance decreases when magnitude of injected current is increased. The decrement rate is more for high soil resistivity as compared to the low soil resistivity. From Fig. 4a, it can be observed that the calculated results are in good agreement with the results reported in [14]. Two and four vertical rods with length of 3.05 m each, separated with same distance of its length, are analyzed, and results are compared with [14], and the same is reported in Fig. 4b. Calculated result shows strong agreement with published result. It is observed that consideration of mutual coupling effect gives better result that is approximately equal to the result evaluated in [14] as shown in Fig. 4a, b. For high soil resistivity and high magnitude of injected current, greater reduction in impulse impedance is observed. The analysis of grounding

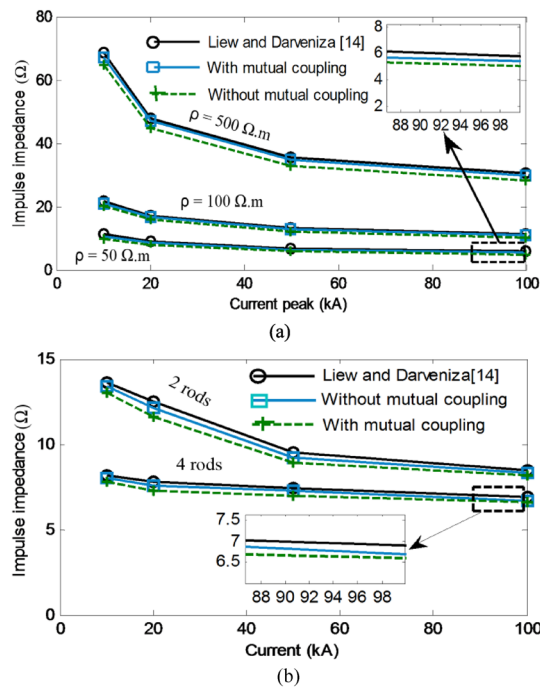


Fig. 4 Impulse impedance variations with current peaks. **a** Single vertical grounding rod buried in different soil resistivity. **b** More than one (2 and 4) vertical grounding rods buried in homogenous soil with $\rho = 100\Omega\text{m}$

Table 1 Comparison of impulse impedance for single vertical rod with and without consideration of mutual coupling

Current peak (kA)	Soil resistivity								
	$\rho = 50 \Omega \text{ m}$			$\rho = 100 \Omega \text{ m}$			$\rho = 500 \Omega \text{ m}$		
	Impulse impedance (Ω)		Relative difference (in %)	Impulse impedance (Ω)		Relative Difference (in %)	Impulse impedance (Ω)		Relative difference (in %)
	With mutual coupling	Without mutual coupling		With mutual coupling	Without mutual coupling		With mutual coupling	Without mutual coupling	
10	10.51	10.00	4.85	21.00	20.20	3.81	67.00	65.00	2.98
20	8.50	8.00	5.88	16.60	15.80	4.82	47.00	45.00	4.25
50	6.40	6.00	6.25	12.70	12.00	5.51	34.80	33.00	5.17
100	5.42	5.00	7.75	11.00	10.20	7.27	30.00	28.40	5.33

system impulse impedance is made for both, with and without considering mutual coupling effect. The percentage relative difference between them is evaluated and reported in Tables 1 and 2 for grounding system with single vertical rod and two and four vertical rods, respectively.

Validation with Zhiqiang Feng et.al. [25]

In this sub-section, the grounding systems considered for the validation of developed method are as follows;

Table 2 Comparison of impulse impedance of more than one vertical grounding rod with and without consideration of mutual coupling for $\rho = 100 \Omega \cdot \text{m}$

Current peak (kA)	Two vertical rods			Four vertical rods		
	Impulse impedance (Ω)		Relative difference (in %)	Impulse impedance (Ω)		Relative difference (in %)
	With mutual coupling	Without mutual coupling		With mutual coupling	Without mutual coupling	
10	13.40	13.00	2.98	8.00	7.80	2.50
20	12.10	11.60	4.13	7.60	7.30	3.94
50	9.20	8.70	5.43	7.30	7.00	4.11
100	8.20	7.70	6.10	6.80	6.40	5.88

- (i) Single horizontal grounding electrode
- (ii) Square grounding electrode

The grounding electrodes are made of solid round steel and buried in homogenous soil with the soil resistivity of $120 \Omega \cdot \text{m}$. The burial depth of the grounding electrodes is 0.08 m . The critical breakdown field strength E_c of soil is considered as 92.58 kV/m .

Single horizontal grounding electrode (Different electrode length)

Various lengths of the electrode are considered in this study as reported in [49]. The length of electrode is $1.0, 1.2, 1.6$ and 2.0 m with radius of 0.12 cm . The peak of injected impulse current I_m is 0.2 kA , wave-front time t_f is $0.35\text{--}0.50 \mu\text{s}$, and time to half value t_f is $150\text{--}250 \mu\text{s}$. Figure 5 shows calculated impulse impedance using developed model for different electrode length. It is observed that the calculated results are in good agreement with results reported in [25]. Impulse impedance decreases when the length of the horizontal grounding electrode is increased. A comparison between measured impulse impedance and calculated impulse impedance was performed, and errors between them are computed using (27)

$$\text{error}(\delta) = \frac{Z_m - Z_c}{Z_m} \times 100\% \quad (27)$$

where Z_m is measured impulse impedance, and Z_c is calculated impulse impedance. The calculated results using developed method are close to the measured results. Calculated errors for different electrode lengths of horizontal grounding electrodes are less than 7% and reported in Fig. 6 that shows the efficacy of developed model.

Square horizontal grounding electrode

A square grounding electrode with side length of 0.45 m and radius of 0.25 cm is buried in the homogenous soil. The injected impulse current magnitude varies from 88 to 700 A and injected at corner of the square electrode. The wave-front time and time to half value of injected impulse current are $0.35\text{--}0.50 \mu\text{s}$ and $150\text{--}250 \mu\text{s}$, respectively. Figure 6 shows calculated grounding impulse impedance for different magnitude of impulse current. Impulse impedance decreases when the magnitude of injected current is increased. A comparison between measured impulse impedance and calculated impulse impedance

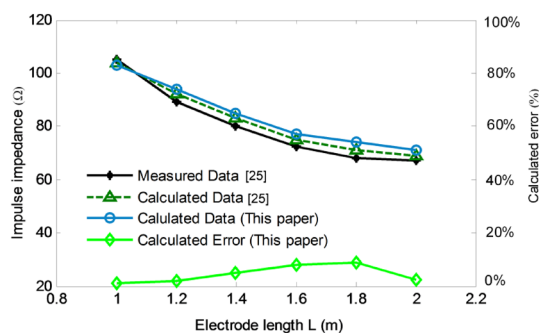


Fig. 5 Impulse impedance and error analysis for horizontal grounding electrode for different electrode length

was done, and errors are computed for different magnitude of impulse current using (28). Obtained error is less than 6% as reported in Fig. 6. Calculated results show the strong agreement with measured and calculated results reported in [25].

Implementation of the developed method

The developed method for impulse impedance calculation described in Sect. "Validation of the method" is further considered here as an application for analyzing horizontal grounding electrodes and grounding grids. A horizontal electrode and a grounding grid shown in Fig. 7a, b, respectively, are considered to analyze the effect of injected impulse current on impulse impedance. The dimension of grounding grid is 4 m × 4 m. The numbers of meshes in the grid are 4 with the dimension of 1 m × 1 m each. Horizontal electrode and grid both are made by copper conductors with 10 mm radius and buried in homogeneous soil at 1 m depth. A 4 μs time-to-peak ramp current wave of different magnitude is injected and impulse impedances are calculated. Comparison results of impulse impedance with and without consideration of mutual coupling between the conductors are shown in Fig. 8a, b for horizontal conductor and grounding grid, respectively. Tables 3 and 4 represent the percentage relative difference in the impulse impedance for horizontal conductor and grid, respectively. From the analysis, it is observed that impulse impedance is increased when mutual effects between the conductors are considered. For low resistivity soil mutual

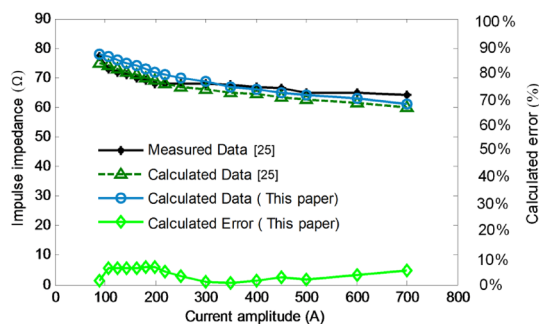


Fig. 6 Impulse impedance and error analysis for square grounding electrode for different current amplitude

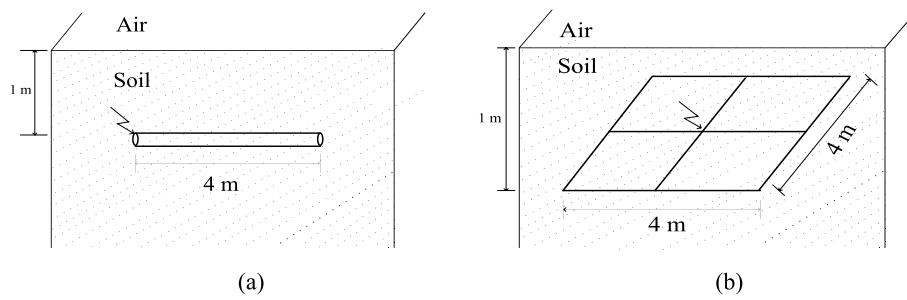


Fig. 7 Grounding system for analysis, **a** horizontal conductor, **b** grounding grid

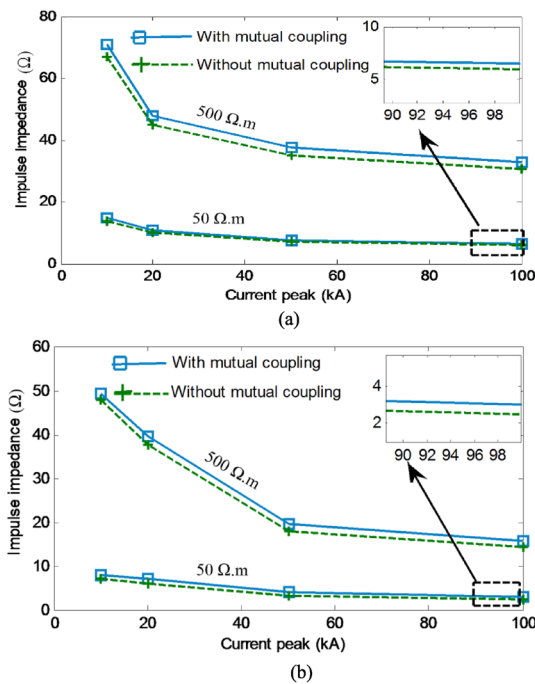


Fig. 8 Impulse impedance variations with current peaks for different soil resistivity, **a** for horizontal conductor, **b** for grounding grid

Table 3 Comparison of impulse impedance of horizontal grounding conductor with and without considering the mutual coupling

Current Peak (kA)	Soil Resistivity					
	$\rho = 50 \Omega \text{ m}$			$\rho = 500 \Omega \text{ m}$		
	Impulse impedance (Ω)		Relative difference (in %)	Impulse impedance (Ω)		Relative difference (in %)
	With mutual coupling	Without mutual coupling		With mutual coupling	Without mutual coupling	
10	14.70	13.80	6.12	71.00	67.00	5.63
20	10.70	10.00	6.54	48.00	45.00	6.25
50	7.60	7.00	7.89	37.60	35.00	6.91
100	6.60	6.00	9.09	33.00	30.60	7.27

Table 4 Comparison of impulse impedance of grounding grid with and without considering the mutual coupling

Current peak (kA)	Soil resistivity					
	$\rho = 50 \Omega \cdot m$			$\rho = 500 \Omega \cdot m$		
	Impulse impedance (Ω)		Relative difference (in %)	Impulse impedance (Ω)		Relative difference (in %)
	With mutual coupling	Without mutual coupling		With mutual coupling	Without mutual coupling	
10	8.00	7.20	10.00	49.20	48.00	2.44
20	7.00	6.10	12.86	39.70	37.60	5.29
50	3.90	3.30	15.38	19.60	18.00	8.16
100	3.00	2.50	16.67	15.60	14.20	8.97

phenomenon is more effective than high resistivity soil. Greater reduction in impulse impedance is seen when high magnitude current is injected on grounding system buried in higher soil resistivity. Percentage relative difference of impulse impedance is large for high magnitude current. Mutual coupling phenomenon is more effective during the injection of high magnitude impulse current. From Tables 1, 3 and 4, it is observed that the percentage relative difference between the impulse impedance with and without considering the coupling effect is reduced for increasing soil resistivity with the same peak of injected current. Impulse impedance depends on the shape and size of the grounding system. At $\rho = 50\Omega m$ and current peak of 10kA, impulse impedance for single vertical rod is 10.51 Ω , for horizontal conductor is 14.70 Ω and for grounding grid is 8.00 Ω . For a particular grounding system at constant resistivity, percentage relative difference of impulse impedance is increased with increases in the injected impulse current peak.

Transient voltage calculation at different points of the grounding system

Comparison with Jose Cidras et.al. [15]

A square grounding grid with the dimensions of 20 m \times 20 m as shown in Fig. 9 was considered for the transient analysis [15]. The grid is made by copper conductors with 10 m.m diameter and buried in homogenous soil at the depth of 1 m from the soil surface. The soil resistivity is 100 $\Omega \cdot m$, and permeability is 10. The critical electric field E_c is considered as 100 kV/m. The grid is excited by 6/20 μs impulse current wave with 50 kA peak value. Current impulse is injected at point O, and generated voltage is calculated at points O, C and B. Figure 10 shows the simulated voltage at given points and comparison with the results reported in [15].

The differences between voltage peaks at the same point with and without consideration of soil ionization are large and decrease at far point from injection point. From Fig. 10, it is observed that generated potential at point O(current injection point) is close to the result given in [15], but differ at points C and B. This is due to the inductive coupling that is considered in the developed model but not considered in the model proposed in [15].

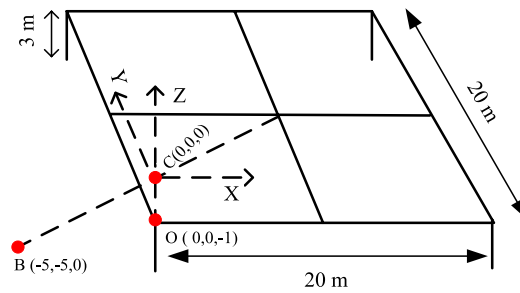


Fig. 9 Grounding grid for analysis

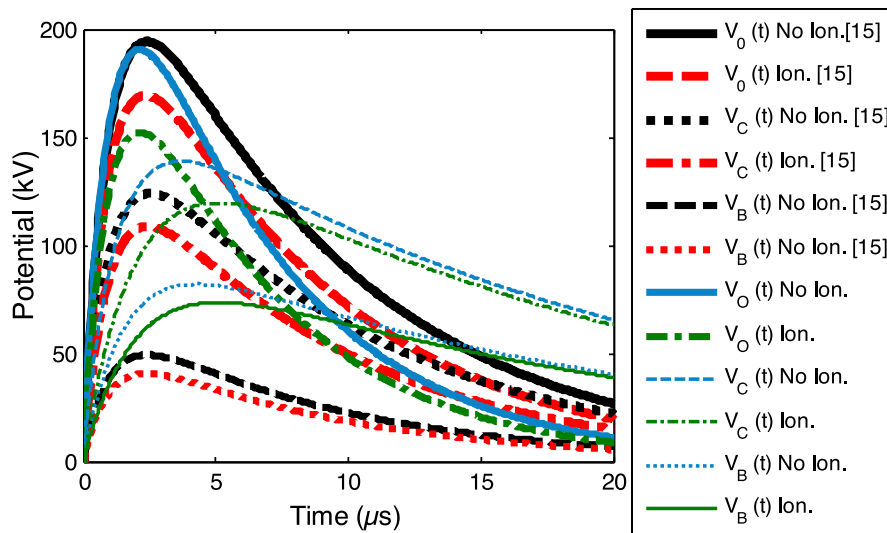


Fig. 10 Simulated voltages at different points of grounding system (O, C, and B) and comparison with the results reported in [15]

Table 5 Comparison of impulse impedance for different length of horizontal grounding electrodes buried in soil at 0.8 m depth with and without consideration of mutual coupling

Grounding Electrode Length (m)	Current peak (kA)								
	10 (kA)			20 (kA)			50 (kA)		
	Impulse Impedance (Ω)			Impulse Impedance (Ω)			Impulse Impedance (Ω)		
	With mutual coupling	Without mutual coupling	Relative difference (in %)	With mutual coupling	Without mutual coupling	Relative difference (in %)	With mutual coupling	Without mutual coupling	Relative difference (in %)
5	75.4	70.3	6.8	67.4	62.0	8.0	60.9	55.4	9.0
10	51.2	47.2	7.8	46.2	42.0	9.1	40.3	36.0	10.6
20	33.0	30.1	8.8	26.0	23.2	10.7	22.6	20.0	11.5
30	24.3	22.0	9.4	19.4	17.2	11.3	17.1	15.0	12.2
50	18.9	17.0	10.0	15.9	14.0	11.9	13.6	11.9	12.2

Influence of grounding electrode length on impulse impedance

Different length of horizontal grounding electrode is considered in this sub-section to simulate the effects of conductor length on impulse impedance. Grounding electrodes are made by copper conductors of radius 10 mm and buried in homogenous soil at the depth

of 0.8 m from the soil surface. The soil resistivity is 500 Ω m. 10 kA, 20 kA, and 50 kA current peak with 2.6 μ s wave-front time are injected on the grounding electrode and impulse impedance that are calculated. Comparison results of impulse impedance with and without consideration of mutual coupling effects are represented in Table 5. From the analysis, it is observed that for high impulse current peak, mutual coupling phenomenon is more effective than low current peak. When length of grounding electrode is increased, the impulse impedance is decreases. Percentage difference between the impulse impedance with and without considering the coupling effect is increased for long grounding electrode with same current peak.

Conclusion

A modified model is used to simulate the transient performance of the grounding system during leakage of high magnitude current into the soil. Proposed model includes coupling phenomenon between the grounding electrodes and frequency-dependent impedance. Test case (single vertical rod, horizontal and square grounding electrode) results obtained using the proposed method are in good agreement with the literature. Furthermore, a horizontal conductor and grounding grids are used to apply this model, and satisfactory results are obtained. Transient voltages at different points of the grounding system are calculated with and without consideration of soil ionization phenomenon, and simulated results are compared with the published results. It is observed that consideration of mutual coupling between the grounding electrodes give more satisfactory results as compared to ignore the mutual coupling. Percentage relative difference is calculated in impulse impedance analysis. For higher magnitude current and higher soil resistivity, rate of reduction in grounding impulse impedance is more. Proposed model assumes that the grounding grid consists of cylindrical conductors. For noncylindrical conductors, grounding electrodes can be represented by equivalent cylindrical conductors which are possible determined rigorously. Also, this method is not effective for large length of grounding conductors. For future work, experimental studies could be conducted at the field test site on the frequency-dependent electrical soil parameters to develop a greater understanding of the characteristics of grounding systems under high frequency and low/high current impulse.

Acknowledgements

The authors thank the Department of Electrical Engineering, NIT Raipur, for providing the facilities and support to conduct this research work.

Author contributions

In this paper, KPS develops methodology for transient analysis of grounding electrode and did simulation work. KC validates the results with the published works.

Funding

There is no funding for this research work.

Availability of data and materials

For the proposed method and validation of the simulated results, data set is taken from published articles. These articles are cited in the manuscript properly. I hope publication will find the cited paper in the reference section positively. Some data are generated during the study that Authors do not wish to share.

Declarations

Competing interests

Authors have no conflict of interest.

Received: 4 July 2023 Accepted: 18 October 2023

Published online: 14 November 2023

References

1. Guo Z, Wu G, Chen S, Zhang Y, Wei W (2018) Transient Behavior of common grounding grids to artificially triggered lightning. *IEEE Trans Electromagn Compat* 61(2):426–433
2. Mazzetti C (2003) Principles of protection of structures against lightning. In: Cooray V (ed) *The lightning flash*. IEE, London, U.K., pp 503–548
3. Sengar KP, Chandrasekaran K (2019) Designing of cost minimum substation grounding grid system using DE, SCA, and HDESCA techniques. *IET Sci Meas Technol* 13(9):1260–1267
4. Sengar KP, Chandrasekaran K (2018) Effects of cost optimised grid configuration on earthing system performance: a comparative assessment. *IET Sci Meas Technol* 14(5):610–620
5. Standard 80, I.E.E.E: IEEE guide for safety in AC substation grounding' (New York, USA, 2000).
6. Zhang B, He J, Lee JB, Cui X, Zhao Z, Zou J (2005) Numerical analysis of transient performance of grounding systems considering soil ionization by coupling moment method with circuit theory. *IEEE Trans Magn* 41(5):1440–1443
7. Visacro S (2007) A comprehensive approach to the grounding response to lightning current. *IEEE Trans Power Deliv* 22(1):381–386
8. Visacro S, Alipio R (2012) Frequency dependence of soil parameters: experimental results, predicting formula and influence on the lightning response of grounding electrodes. *IEEE Trans on Power Deliv* 27(2):927–935
9. Visacro S, Rosado G (2009) Response of grounding electrodes to impulsive currents: An experimental evaluation. *IEEE Trans Electromagn Compat* 51(1):161–164
10. Zhang B, Zhao Z, Cui X, Li L (2002) Diagnosis of breaks in substation's grounding grid by using the electromagnetic method. *IEEE Trans Magn* 38(2):473–476
11. Xiong R, Chen B, Han JJ, Qiu YY, Yang W, Ning Q (2012) Transient resistance analysis of large grounding systems using the FDTD method. *Progress Electromagn Research* 132:59–175
12. Li J, Yuan Y, Yang Q, Sima W, Sun C, Zahn M (2011) Numerical and experimental investigation of grounding electrode impulse-current dispersal regularity considering the transient ionization phenomenon. *IEEE Trans Power Deliv* 26(4):2647–2658
13. Chen H, Du Y (2019) Lightning grounding grid model considering both the frequency-dependent behavior and ionization phenomenon. *IEEE Trans Electromagn Compat* 61(1):157–165
14. Liew AC, Darveniza M (1974) Dynamic model of impulse characteristics of concentrated earths. *IEE Proc* 121(2):123–135
15. Cidras J, Otero AF, Garrido C (2000) Nodal frequency analysis of grounding systems considering the soil ionization effect. *IEEE Trans Power Deliv* 15(1):103–107
16. Mousa AM (1994) The soil ionization gradient associated with discharge of high currents into concentrated electrodes. *IEEE Trans Power Deliv* 9(3):1669–1677
17. Liu Y, Theethayi N, Thottappillil R (2005) An engineering model for transient analysis of grounding system under lightning strikes: nonuniform transmission-line approach. *IEEE Trans Power Del* 20(2):722–730
18. Mokhtari A-M, Z, Salam Z, (2015) An improved circuit-based model of a grounding electrode by considering the current rate of rise and soil ionization factors. *IEEE Trans Power Deliv* 30(1):211–219
19. Tong X, Dong X, Tan B (2019) High current field test of impulse transient characteristics of substation grounding grid. *J Eng* 16:2018–2021
20. Permal N, Osman M, Kadir MZAA, Ariffin AM (2020) Review of substation grounding system behavior under high frequency and transient faults in uniform soil. *IEEE Access* 8:142468–142482
21. Mohamad Nasir NAF, Ab Kadir MZA, Osman M, Abd Rahman MS, Ungku Amirulddin UA, Mohd Nasir MS, Nik Ali NH (2021) Influence of lightning current parameters and earthing system designs on tower footing impedance of 500 kV lines. *Energies* 14(16):4736
22. Harid N, Griffiths H, Mousa S, Clark D, Robson S, Haddad A (2015) On the analysis of impulse test results on grounding systems. *IEEE Trans Ind Appl* 51(6):5324–5334
23. Kherif O, Chiheb S, Teguvar M, Mekhaldi A, Harid N (2018) Time-domain modeling of grounding systems impulse response incorporating nonlinear and frequency-dependent aspects. *IEEE Trans Electromagn Compat* 60(4):907–916
24. Zeng R, Gong X, He J, Zhang B, Gao Y (2008) Lightning impulse performances of grounding grids for substations considering soil ionization. *IEEE Trans Power Del* 23(2):667–675
25. Feng Z, Wen X, Tong X, Lu H, Lan L, Xing P (2015) Impulse characteristics of tower grounding devices considering soil ionization by the time-domain difference method. *IEEE Trans Power Del* 30(4):1906–1913
26. Boutadjine A, Nekhoul B (2022) Realistic modeling of the grounding system transient behavior with frequency dependence. *Electr Power Syst Res* 203:107644
27. Nekhoul B, al. (2022) A simplified numerical modeling of the transient behavior of grounding systems considering soil ionization. *Electric Power Syst Res* 211:108182
28. Qi L, Cui X, Zhao Z, Li H (2006) Grounding performance analysis of the substation grounding grids by finite element method in frequency domain. *IEEE Trans Magn* 43(4):1181–1184
29. Karami H, Sheshyekani K, Rachidi F (2017) Mixed-potential integral equation for full-wave modeling of grounding systems buried in a lossy multilayer stratified ground. *IEEE Trans Electromagn Compat* 59(5):1505–1513
30. Grcev L, Dawalibi F (1990) An electromagnetic model for transients in grounding systems. *IEEE Trans Power Del* 5(4):1773–1781
31. Grcev L (2009) Modeling of Grounding Electrodes Under Lightning Currents. *IEEE Trans Electromagn Compatibil* 51(3):1
32. Nekhoul B et al (1996) Calculating the impedance of a grounding system. *IEEE Trans Magn* 32(3):1
33. de Lima ACS, Portela C (2007) Inclusion of frequency-dependent soil parameters in transmission-line modelling. *IEEE Trans Power Del* 22(1):492–499
34. Gazzana DS, Bretas AS, Dias GA, Telló M, Thomas DW, Christopoulos C (2014) The transmission line modeling method to represent the soil ionization phenomenon in grounding systems. *IEEE Trans Magn* 50(2):505–508

35. Li Z-X, Ke-Li G, Rao S-W (2020) Lightning response of a grounding system buried in multiple layers in earth using the PEEC method based on the quasi-static complex image method. *Electric Power Components Syst* 48(3):291–303
36. Ghomi M, da Silva FF, Akmal AAS, Bak CL (2022) Transient overvoltage analysis in the medium voltage substations based on full-wave modeling of two-layer grounding system. *Electric Power Syst Res* 211:108139
37. Da Silva WC, De Azevedo WLM, D'Annibale JLA, De Araújo ARJ, Pissolato Filho J (2023) Transient analysis on wind farms with interconnected grounding systems located on frequency-dependent soils. In: 2023 IEEE Power & Energy Society General Meeting (PESGM). IEEE, pp 1–5
38. Harrington RF (1993) *Field computation by moment methods*. Wiley-IEEE Press
39. Sunde ED (1949) *Earth conduction effect in transmission system* Bell Telephonic Laboratories Incorporated, pp 146–148
40. Grover FW (1962) *Inductance calculations*. Dover Publications, New York
41. Ruehli AE, Antonini G, Jiang LJ (2013) Skin-effect loss models for time-and frequency domain PEEC solver. *Proc IEEE* 101(2):451–472
42. Chen H, Du Y (2018) Model of ferromagnetic steels for lightning transient analysis. *IET Science, Meas & Tech* 12(3):301–307
43. Paul CR (2011) *Inductance: loop and partial*. Wiley
44. Zhiwei L, Zhao Z (2012) The grounding impedance calculation of large steel grounding grid". *Energy Procedia* 17(2013):157–163
45. CIGRE Working Group on Lightning (1991) *Guide to procedures for estimating the lightning performance of transmission lines*. CIGRE, Paris
46. Oettle EE (1988) A new general estimation curve for predicting the impulse impedance of concentrated earth electrodes. *IEEE Trans Power Deliv* 3(4):2020–2029
47. Wang J, Liew AC, Darveniza M (2005) Extension of dynamic model of impulse behavior of concentrated grounds at high currents. *IEEE Trans Power Del* 20(3):2160–2165
48. Poljak D, Doric V (2006) Wire antenna model for transient analysis of simple grounding systems, Part I: The vertical grounding electrode. *Progress Electromagn Res* 64:149–166
49. Sekioka S, Sonoda T, Ametani A (2005) Experimental study of current-dependent grounding resistance of rod electrode. *IEEE Trans Power Deliv* 20(2):1569–1576

Publisher's Note

Springer Nature remains neutral with regard to jurisdictional claims in published maps and institutional affiliations.